nature physics

SUPPLEMENTARY INFORMATION
https://doi.org/10.1038/s41567-017-0008-5

In the format provided by the authors and unedited.

Quantum violation of an instrumental test

Rafael Chaves [1]*, Gonzalo Carvacho [2], Iris Agresti [2], Valerio Di Giulio [2], Leandro Aolita [3], Sandro Giacomini [2] and Fabio Sciarrino [2]*

[1]International Institute of Physics, Federal University of Rio Grande do Norte, 59078-970, PO BOX 1613, Natal, Brazil. [2]Dipartimento di Fisica - Sapienza Università di Roma, P.le Aldo Moro 5, 00185 Roma, Italy. [3]Instituto de Física, Universidade Federal do Rio de Janeiro, Caixa Postal 68528, Rio de Janeiro, RJ 21941-972, Brazil. *e-mail: rchaves@iip.ufrn.br; fabio.sciarrino@uniroma1.it

Supplementary Information: Quantum Violation of an Instrumental Test

Rafael Chaves,[1,*] Gonzalo Carvacho,[2] Iris Agresti,[2] Valerio Di Giulio,[2] Leandro Aolita,[3] Sandro Giacomini,[2] and Fabio Sciarrino[2,†]

[1]*International Institute of Physics, Federal University of Rio Grande do Norte, 59078-970, P. O. Box 1613, Natal, Brazil*
[2]*Dipartimento di Fisica - Sapienza Università di Roma, P.le Aldo Moro 5, I-00185 Roma, Italy*
[3]*Instituto de Física, Universidade Federal do Rio de Janeiro, Caixa Postal 68528, Rio de Janeiro, RJ 21941-972, Brazil*

(Dated: October 4, 2017)

Geometric description of the set of classical correlations in the instrumental DAG

As discussed in the main text, the Markov condition for the instrumental DAG implies that any observable probability distribution compatible with it can be decomposed as

$$p(a,b|x)=\sum_{\lambda}p(a|x,\lambda)p(b|a,\lambda)p(\lambda). \tag{1}$$

As we can see, this decomposition defines a convex set (the convex sum over the probabilities for the variable Λ). For discrete variables, this set is in fact a polytope, that is, a convex set with finitely many extremal points and that can be equivalently described by finitely many linear inequalities that represent the boundaries of the polytope (from which the non-trivial represent instrumental inequalities).

As mentioned in the main text, the probabilities appearing in the decomposition above can without loss of generality be expressed as deterministic (response) functions. More precisely, we have that

$$a=D_a(x,\lambda), \tag{2}$$
$$b=D_b(a,\lambda). \tag{3}$$

That is, for a given value of λ the variable a is a deterministic function of x; similarly b is a deterministic function of a. We can think of the variable λ as selecting which function to use in a given run of the physical process (with probability $p(\lambda)$). The number of possible deterministic functions to choose from will intrinsically depend on the domain of the variables. Namely, the number of deterministic functions for variable A is given by $|a|^{|x|}$ and for variable B is given by $|b|^{|a|}$, where $|a|$ is the number of values taken by the random variable A (similarly for B and X). Thus the total number of deterministic functions is given by $|a|^{|x|}|b|^{|a|}$; each of these corresponding to one of the extremal points defining the convex set defined by (1).

Given the list of extremal points of a polytope, we can find its dual description in terms of facets, that is, linear inequalities of the probabilities $p(a,b|x)$ that generically can be written as

$$\sum_{a,b,x}c_{a,b,x}p(a,b|x)\leq B_{\text{Classical}}, \tag{4}$$

where $c_{a,b,x}$ are real coefficients and $B_{\text{Classical}}$ corresponds to the maximum values achievable by the extremal points. Further, this dualization procedure can be performed using standard convex optimization software [1]. A given correlation is compatible with the instrumental DAG if and only if it respects all of these inequalities. If any of them is violated we thus have an unambiguous proof that some of the causal assumptions is incompatible with the correlation under test.

Quantum and post-quantum violations of the instrumental inequality

Our interest is to find the optimal quantum violations of inequality (eq. (6) in the main text)

$$\mathcal{I}=-\langle B\rangle_1+2\langle B\rangle_2+\langle A\rangle_1-\langle AB\rangle_1+2\langle AB\rangle_3\leq 3,. \tag{5}$$

That is, to find the optimal quantum state and measurements producing correlations according to

$$p_Q(a,b|x)=\mathrm{Tr}\left[(M_a^x\otimes M_b^a)\varrho\right]. \tag{6}$$

To that aim we have restricted our attention to pure two-qubit states of the form $|\Psi\rangle=\cos(\theta)|\uparrow\uparrow\rangle+\sin(\theta)|\downarrow\downarrow\rangle$ (because of the convexity of the set of quantum correlations we do not need to consider mixed states in the optimization). As for the measurement observables we have considered qubit projective measurements. Thus, the variable A is associated to the measurement outcome of the measurement performed on the first qubit of the pair and, following the prescription of the instrumental DAG, the measurement settings for the second qubit (the measurements outcomes which correspond to the variable B) can depend on the measurement outcome of the first measurement. By numerically optimizing (in Mathematica) the measurement settings for each value of θ we observe that

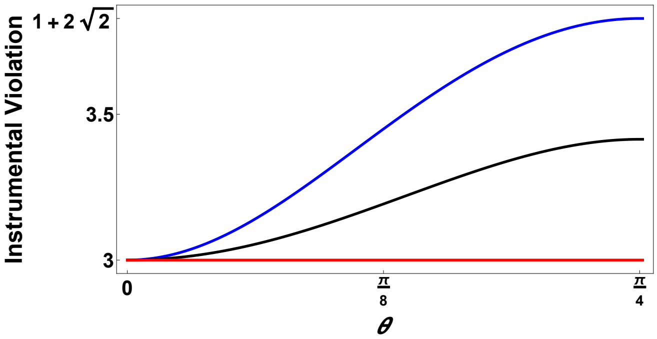

FIG. 1. **Violation of the instrumental inequality** (5) **as function of** θ**:** every pure entangled state violates the inequality and the maximum is achieved by the maximally entangled state. The blue curve shows the optimal violation obtained numerically by considering projective measurements on both qubits. The black curve shows the (non-optimal) violation following (7). The red line shows the classical limit.

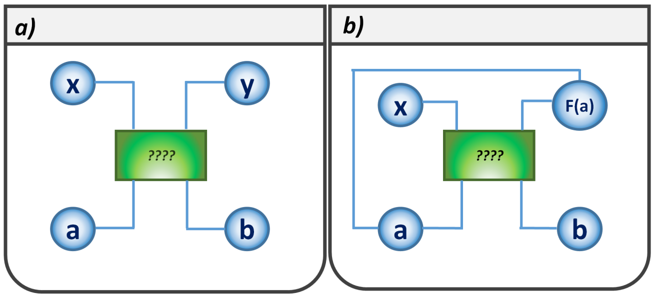

FIG. 2. **Black-box representation of a physical process:** a) The black box associated to a probability distribution $p(a,b|x,y)$. b) The wired box used to produce the probability $p(a,b|x)$.

every entangled state ($\theta \neq n\pi/2$) violates the inequality and that the maximal violation is obtained for maximally entangled states ($\theta = \pi/4$) (see Fig. 1).

To prove analytically that every entangled pure state of two-qubits (considering without loss of generality $0 < \theta \leq \pi/4$) violates the inequality it is enough to set $O^{x=1} = -(\sigma_X + \sigma_Z)/\sqrt{2}$, $O^{x=2} = \sigma_X$ and $O^{x=3} = \sigma_Z$ for the first qubit (producing the outcome a) and $O^{a=0} = (\cos(\theta)\sigma_Z + \sin(\theta)\sigma_X)$ and $O^{a=1} = \sigma_Z$ for the second qubit (producing the outcome b). The corresponding value for inequality (5) is given by

$$\frac{1}{4}(4 + (8+3\sqrt{2})\cos(\theta) - 2\sqrt{2}\cos(2\theta) - \sqrt{2}\cos(3\theta)), \tag{7}$$

that can be easily seen to be larger than 3 for any $0 < \theta \leq \pi/4$ (see Fig. 1). We notice that this choice of parameters does not lead to the optimal violation for a given θ but it is enough for the purpose of showing violations.

Instead of considering quantum resources, we can consider what is the maximum violation of the instrumental inequality provided by non-signalling (post-quantum) resources. To that aim, consider a given non-signalling (NS) distribution $p_{NS}(a,b|x,y)$ respecting the NS constraints

$$p_{NS}(a|x) = \sum_b p_{NS}(a,b|x,y) = \sum_b p_{NS}(a,b|x,y'),$$
$$p_{NS}(b|y) = \sum_a p_{NS}(a,b|x,y) = \sum_a p_{NS}(a,b|x',y),$$

for all x, x', y, y'.

NS correlations can represented by the black-box process illustrated in Fig. 2. Just as in the classical and quantum cases, one of the inputs of this black-box can depend on the output obtained earlier. That is, in this case we are considering "wirings" of probability distributions [2], as illustrated in Fig. 2. The probability distribution for the instrumental scenario obtainable from NS resources via these wirings is thus given by

$$p(a,b|x) = p_{NS}(a,b|x,f(a)), \tag{8}$$

where $f(a)$ is an arbitrary deterministic function with $|a|$ possible inputs and $|a|$ possible outputs that describes a wiring from Alice's output to Bob's input. In turn, for a fixed $f(a)$ it is a simple linear program (LP) to find what is the maximum violation of the instrumental inequality (5). Since there are finitely many functions $f(a)$ there is also a finite number of LPs one has to solve. Doing that, we obtain that the maximum violation is $\mathcal{I}_{NS} = 5$. The latter is obtained for $f(a) = a$ and with $p_{NS}(a,b|x,y)$ the simple variation of the Popescu-Rohrlich (PR) box [3] shown in Table I.

$p_{NS}(a,b|x,y) =$

$x\backslash y$		0		1	
	$a\backslash b$	0	1	0	1
0	0	$\frac{1}{2}$	$\frac{1}{2}$	$\frac{1}{2}$	$\frac{1}{2}$
	1	0	0	0	0
1	0	$\frac{1}{2}$	0	0	$\frac{1}{2}$
	1	0	$\frac{1}{2}$	$\frac{1}{2}$	0
2	0	$\frac{1}{2}$	0	$\frac{1}{2}$	0
	1	0	$\frac{1}{2}$	0	$\frac{1}{2}$

TABLE I. A matrix representation of the non-signalling distribution maximally violating the instrumental inequality. The rows stand for the x and a values while the columns stand for y and b. For $x = 0$ we see that A always outputs $a = 0$ while B produces a random bit b. Restricting to the inputs $x = 1, 2$ and transforming them as $x = 1 \rightarrow x = 0$ and $x = 2 \rightarrow x = 1$ we have a symmetry of the PR-box given by $p(a,b|x,y) = \frac{1}{2}\delta_{a\oplus b,(x+1)y}$.

Quantifying causal relaxations in the instrumental DAG

Observed a violation of an instrumental inequality it is natural to consider by how much we have to relax the underlying causal assumptions of the instrumental model in order to explain the observed correlations. As discussed in the main text, the instrumental DAG subsumes two causal assumptions: i) the independence of the instrumental variable X from the hidden variable Λ ($p(x,\lambda) = p(x)p(\lambda)$) and ii) the fact that all the correlations between X and B are mediated via A and Λ ($p(b|a,x,\lambda) = p(b|a,\lambda)$).

The graphical language of DAGs immediately allows us to represent the causal relaxations in both cases (see Fig. 3). In the first case, we allow for correlations between X and Λ to be mediated by a common ancestor Γ. In turn, in the second DAG we allow for a direct causal influence (a directed edge) between variables X and B. The DAG representation, however, do not specify the strength of the arrows, that is, by how much we have the relax the corresponding causal assumptions. To that aim, we first have to introduce a measure of correlations and/or direct causal influence. Below we introduce the measures we consider and using the techniques developed in [4] show how they can be estimated from given observed correlations via a linear program.

For the first case, the observed probability distribution has a decomposition given by

$$p(a,b|x) = \sum_{\lambda,\gamma} p(a|x,\lambda)p(b|a,\lambda)p(\lambda,\gamma|x) \tag{9}$$
$$= \frac{1}{p(x)} \sum_{\lambda,\gamma} p(a|x,\lambda)p(b|a,\lambda)p(\lambda|\gamma)p(x|\gamma)p(\gamma).$$

Without loss of generality, we model such correlations by introducing an additional hidden variable Γ which serves as a common ancestor for X, and Λ. This suggests to decompose this common ancestor into $\gamma = (\gamma_x, \gamma_\lambda)$. We can assume $x = \gamma_x$ and $\lambda = \gamma_\lambda$ (that is, they are deterministic functions) without loss of generality. If the observable variables a, b and x are discrete variables then finitely many different instances of γ suffice to fully characterize the common ancestor's influence.

Alternatively, we can represent (9) as

$$\mathbf{p} = T\mathbf{q}, \tag{10}$$

where $p(a,b|x)$ is represented by a vector $\mathbf{p}$ with components $\mathbf{p}_j$ labeled by the indexes $j = (a,b,x)$ and the distribution of γ is associated with a vector with components $\mathbf{q}_\gamma = p(\Gamma = \gamma)$. In turn, T is a matrix with elements $T_{j,\gamma} = \frac{1}{p(x)}\delta_{x,\gamma_x}\delta_{a,D_a(x,\gamma_\lambda)}\delta_{b,D_b(a,\gamma_\lambda)} = \frac{1}{p(x)}\delta_{a,D_a(\gamma_x,\gamma_\lambda)}\delta_{b,D_b(a,\gamma_\lambda)}$.

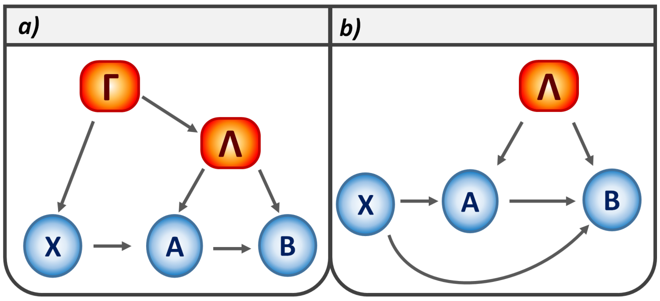

FIG. 3. **Causal relaxations of the instrumental DAG:** a) Measurement independence relaxation where the hidden variable Λ is allowed to be correlated with the instrumental variables X. b) A relaxation where a direct causal influence from X into B is allowed.

Since the correlations between X and Λ are mediated by a third variable Γ, it is reasonable to consider as a measure of correlations the total variation distance given by

$$\mathcal{M}_{X:\Lambda} = \sum_{x,\lambda} |p(x,\lambda) - p(x)p(\lambda)|. \tag{11}$$

There are certainly other good measures one can employ, however, the total variation distance has the good advantage of providing a non-trivial lower bound, via the Pinsker inequality [5], to the mutual information between X and Λ:

$$I(X:\Lambda) \geq \frac{1}{2}\mathcal{M}^2_{X:\Lambda} \log \mathbf{e}, \tag{12}$$

a quantity that is highly non-linear as a function of the probabilities and thus can in practice only be estimated numerically.

In the second case (the one discussed in the main text), we want to quantify the causal influence of the arrow $X \to B$, that is, the causal model allows for distributions $p(a,b|x)$ of the form

$$p(a,b|x) = \sum_{\lambda} p(a|x,\lambda)p(b|a,x,\lambda)p(\lambda). \tag{13}$$

Similarly to what we have done in the case of measurement dependence, we can represent this model as

$$\mathbf{p} = W\mathbf{q}, \tag{14}$$

where again $p(a,b|x)$ is represented by a vector $\mathbf{p}$ with components $\mathbf{p}_j$ labeled by the indexes $j = (a,b,x)$ and the distribution of λ is associated with a vector with components $\mathbf{q}_\lambda = p(\Lambda = \lambda)$. In turn, W is a matrix with elements $W_{j,\lambda} = \delta_{a,D_a(x,\lambda)}\delta_{b,D_b(a,x,\lambda)}$.

Since in this case we do have a direct arrow between the variables, it is more appropriate to consider a measure of causal influence rather than a simple measure of correlations. As discussed in the main text, in this case we consider the measure of causal influence defined as

$$\mathcal{C}_{X\to B} = \sup_{x,x',a,b} \sum_{\lambda} p(\lambda)|p(b|a,do(x),\lambda) - p(b|a,do(x'),\lambda)|. \tag{15}$$

Further, we notice that in this case, since the variables X and B have no common ancestors, the intervention (the do operation) is totally equivalent to a simple conditional operation, that is, $p(b|do(x)) = p(b|x)$ and thus

$$\mathcal{C}_{X\to B} = \sup_{x,x',a,b} \sum_{\lambda} p(\lambda)|p(b|a,x,\lambda) - p(b|a,x',\lambda)|. \tag{16}$$

Given some observed probability distribution or given the violation of some instrumental inequality (represented by a given matrix V such that $V\mathbf{p}$ gives the corresponding inequality), our aim is to estimate the minimum relaxation necessary to explain it. In other terms what is the minimum value of $\mathcal{M}_{X:\Lambda}$ or $\mathcal{C}_{X\to B}$. That is, we are interested in the following minimization problems:

$$\begin{aligned} \underset{\mathbf{q}\in\mathbb{R}^n}{\text{minimize}} \quad & \mathcal{M}_{X:\Lambda} && (17)\\ \text{subject to} \quad & VT\mathbf{q} = V\mathbf{p} \\ & \langle \mathbf{1}_n, \mathbf{q}\rangle = 1 && (18)\\ & \mathbf{q} \geq \mathbf{0}_n. \end{aligned}$$

or

$$\begin{aligned} \underset{\mathbf{q}\in\mathbb{R}^n}{\text{minimize}} \quad & \mathcal{C}_{X\to B} && (19)\\ \text{subject to} \quad & VW\mathbf{q} = V\mathbf{p} \\ & \langle \mathbf{1}_n, \mathbf{q}\rangle = 1 && (20)\\ & \mathbf{q} \geq \mathbf{0}_n. \end{aligned}$$

Following the results in [4], these optimization problems can be casted a linear programs and thus analytical and computationally efficient solutions can be found. Notice that the same approach can be applied to compute the average causal effect $\text{ACE}_{A\to B}$ and the direct causal influence $\mathcal{C}_{X\to B}$ (eqs. (1) and (12) of the main text).

A simple example showing how post-selection can simulate non-local correlations

Here we illustrate how in the usual Bell scenario the post-selection of data given by $y = a$ can be used to simulate non-local and signalling correlations through local hidden variable (LHV) models. However, as discussed in the main text such post-selection is allowed if instead of testing quantum mechanics againts LHV models we test it against non-local hidden variable models, more specifically a model where the outcome A has a direct causal influence over Y (thus also allowing for measurement dependence).

Consider the mixture (with equal weights) of two deterministic local strategies such that $p(a,b,x,y) = \frac{1}{4}p(a,b|x,y)$ where for the first strategy we have $a = x$ and $b = 0$ and for the second we have $a = x\oplus 1$ and $b = y$. As shown in the Table II below (using a matrix representation) under the postselection $y = a$ the first strategy is mapped to a distribution such that $p(x,y) = 1/2$ if $x\oplus y = 0$ (0 otherwise) and the second is mapped to a distribution such that $p(x,y) = 1/2$ if $x\oplus y = 1$ (0 otherwise). That is, this post-selection of data generates measurement dependence between the hidden variable (choosing which deterministic strategy to use) and the measurement choices.

Using the two mentioned local deterministic strategies and after the post-selection, we have a distribution $p(a,b,x,y) = \frac{1}{4}p(a,b|x,y) = \frac{1}{4}\delta_{a,y}\delta_{b,y(x\oplus 1)}$ that achieves the maximum violation the CHSH inequality (= 4) and clearly is signalling.

$x\backslash y$		0		1	
	$a\backslash b$	0	1	0	1
0	0	$\frac{1}{4}$	0	$\frac{1}{4}$	0
	1	0	0	0	0
1	0	0	0	0	0
	1	$\frac{1}{4}$	0	$\frac{1}{4}$	0

$\xrightarrow{y=a}$

$x\backslash y$		0		1	
	$a\backslash b$	0	1	0	1
0	0	$\frac{1}{2}$	0	0	0
	1	0	0	0	0
1	0	0	0	0	0
	1	0	0	$\frac{1}{2}$	0

,

$x\backslash y$		0		1	
	$a\backslash b$	0	1	0	1
0	0	0	0	0	0
	1	$\frac{1}{4}$	0	0	$\frac{1}{4}$
1	0	$\frac{1}{4}$	0	0	$\frac{1}{4}$
	1	0	0	0	0

$\xrightarrow{y=a}$

$x\backslash y$		0		1	
	$a\backslash b$	0	1	0	1
0	0	0	0	0	0
	1	0	0	0	$\frac{1}{2}$
1	0	$\frac{1}{2}$	0	0	0
	1	0	0	0	0

TABLE II. The two upper matrices show the matrix representation for the probability distribution $p(a,b,x,y) = \frac{1}{4}p(a,b|x,y)$ of the local deterministic strategy where $a = x$ and $b = 0$ and how it transforms after performing the post-selection where $y = a$. The two lower matrices show the same for the deterministic strategy $a = x\oplus 1$ and $b = y$.

Addressing the $X \to B$ loophole

Differently from a usual Bell scenario, the instrumental causal structure is not subjected to the locality loophole since the measurement outcome A has a direct causal influence over outcome B also implying that in general X and B will be correlated. As we explain below, the instrumental scenario does introduces a new kind of loophole, which can in principle be addressed relying on interventions. Before discussing the loopholes in the instrumental scenario, first we draw parallels with the usual loopholes and meaning of device-independence in a usual Bell scenario.

The term device-independence refers to the fact that we can infer properties of our system of interest without relying on any assumptions about the internal mechanism of our measurement devices. However, still one has to rely on some global assumptions, external to the inner working of the devices. From a causal networks perspective (from which Bell's theorem is a particular case), device-independence refers to the fact once we impose the external mechanisms (the causal relations between the variables), our conclusions are independent of whatever are the internal mechanisms generating the value of a given variable (linear or non-linear response functions, Gaussian or non-Gaussian distributions, etc).

For example, in a usual Bell scenario we associate the violation of a Bell inequality with a device-independent proof that the underlying quantum state is entangled (thus independent of the fact that we have measured a given observable, the dimension of the quantum state, etc). However, to achieve this conclusion we have to impose the locality and measurement independence assumptions. The question is then how can we be sure to fulfill such assumptions in an experiment?

To close the locality loophole we can rely on physical arguments since by invoking special relativity we can assure the locality assumption by measuring particles that are space-like separated. However, the presence of a possible measurement dependence (correlating the choice of observables and the source preparing the system to be measured) cannot be ruled out on a physical ground, thus introducing a loophole that cannot be closed. Clearly, however, measurement independence is an assumption external to the measurement devices. From the perspective of applications (such as cryptography) device-indepedence means that we can trust our results even without knowing our measurement apparatus that can then be treated as a black box. However, we do have to trust that the causal assumptions are being fulfilled otherwise an eavesdropper can easily simulate apparently quantum non-local correlations with classical resources (for example correlating the source and the measurement choices as has been done above).

The same is true for the instrumental scenario. As opposed to the locality loophole in Bell's theorem, the direct causal influence between the variables X and B (not mediated by variable A) cannot be ruled out by physical grounds such as special relatively. However, just as in the Bell case, once an instrumental inequality is violated we do not rely on any assumption about the measurement apparatus but only on external/causal assumptions. For example, in a clinical trial, the variable X would stand for the treatment assigned to a patient (a drug or placebo), A would represent the compliance of the patient (taking or not the treatment) and B would be treatment response. As discussed in the main text, in such a randomized experiment, it is natural to assume that X has not direct influence over B, however, if the patients discover that they are actually receiving placebo treatment, this might not be true anymore. That is, this loophole cannot be conclusively closed (unless interventions are made, see below), the best one can do is to design the best possible experiment (e.g, patients are unaware of the received treatment). Something similar happens with the measurement independence assumption in a Bell test. The best one can do is to improve our experimental trust in the measurement independence, for instance, using cosmic photons [6] or human randomness [7].

Finally, as a potential way of ruling out such loophole one can make use of interventions. Notice that in the instrumental scenario the variables X and B are in general correlated but all these correlations are mediated by the variable A. This means that by intervening on A (thus breaking the incoming causal link from X) the variable X and B should become independent, that is, $p(b|x, \mathrm{do}(a)) = p(b|\mathrm{do}(a))$. However, if under interventions on A we still observe correlations between X and B, this could only be due some direct influence of X into B thus allowing us to detect such causal link. Of course that interventions are device-dependent operations but at least they provide an experimental way to addressing such loopholes.

To illustrate we give a very simple example. Suppose we have a probability distribution achieving the maximum algebraic value of (5) given by $\mathcal{I}_{\max} = 7$. In this case, clearly we need a the direct causal influence $X \rightarrow B$. One way of achieving this value is via a deterministic strategy such that $a = 0 \quad \forall x$ and $b = 1$ if $x = 1$ and $b = 0$ if $x = 2, 3$ (thus A has in fact no causal influence over B). One can easily check that $p(b|x, \mathrm{do}(a)) \neq p(b|\mathrm{do}(a))$ allowing one to conclude that some direct causal influence between X and B is present.

The effect of detection inefficiencies

As it happens with Bell tests, the experimental implementation of the violation of the instrumental inequality is also subjected to experimental imperfections. Here we analyze in details the effects of detections inefficiencies, that is, the fact that some of the generated photons might not lead to a detection click.

In our setup two entangled photons are generated and then measured in a projective basis, that is, defined the measurement direction we have two possible outcomes: 0 (corresponding to the eigenvalue $+1$) and 1 (corresponding to the outcome -1). In this situation, the non-detection of a photon, labelled by $\emptyset$, can be handled by two different approaches.

First, one can treat the no-click event as third possible outcome of the performed measurement. However, notice that the instrumental inequality (5) refers to a scenario where only two outcomes are allowed. Thus, to treat the no-click as third event we have derive new instrumental inequalities taking that into account.

The second possibility, the one we follow here, is to remain in a description with two outcomes only and thus treat the no-click by a binning approach, that is, whenever a non-click happens we simply label $\emptyset$ as either 0 or 1. In this case we can simply use inequality (5).

Quite generally a measurement with two outcomes can be represented by the POVM operators [8]

$$\begin{aligned} M_{\uparrow} &= \eta_{\uparrow}|\uparrow\rangle\langle\uparrow| + (1-\eta_{\downarrow})|\downarrow\rangle\langle\downarrow|, \\ M_{\downarrow} &= \eta_{\downarrow}|\downarrow\rangle\langle\downarrow| + (1-\eta_{\uparrow})|\uparrow\rangle\langle\uparrow|, \end{aligned} \tag{21}$$

where $\eta_{\uparrow} = \eta_{\downarrow} = 1$ represent the case of perfect projective measurements and where $|\uparrow,\downarrow\rangle$ represent some arbitrary basis for qubits.

To model the binning of the no-click event we can make $\eta_{\uparrow} = 1$ and $\eta_{\downarrow} = \eta$ (where η is the detection efficiency of the photon detector). This corresponds to the case where whenever we obtain $\emptyset$ we simply relabel it as the outcome 0 (corresponding to projection in $\uparrow$). In other terms the event $\emptyset$ is binned with the event 0. Using this modeling and optimizing over the entangled states and measurement basis we have obtained the minimum detection efficiencies required to obtain a detection-loophole-free violation of inequality (5). The results are shown in Fig. 4.

We observe that there is an asymmetry between the detection efficiencies of the η_a and η_b corresponding to the measurements outcomes A and B, respectively. Setting $\eta_a = 1$ we obtain the critical value $\eta_b^{\text{crit}} \approx 0.667$, below which no violation of the instrumental inequality is possible anymore. In turn, for $\eta_b = 1$ we observe $\eta_a^{\text{crit}} \approx 0.828$. That is, the violation is more robust according to the detection inefficiencies of the measurement corresponding to the B variable. Instead, if we set $\eta_a = \eta_b = \eta$ we obtain $\eta^{\text{crit}} \approx 0.905$.

Further, we observe that for detection inefficiencies in a, the optimal states are always maximally entangled. In turn, for detection inefficiencies in b, the best violations are obtained by states with reduced entanglement that in fact tend to separable states as $\eta_b \to \eta_b^{\text{crit}}$. This is a similar effect to that in usual Bell tests [9], such that

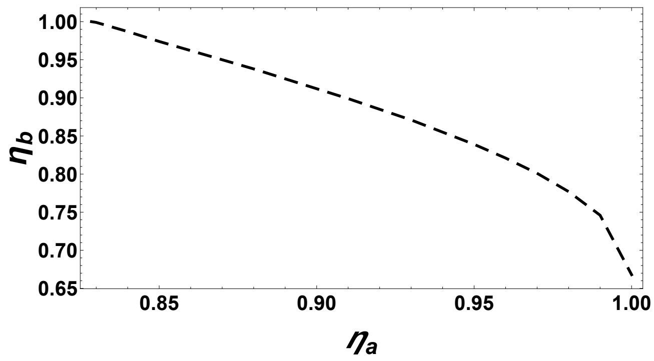

FIG. 4. **Critical values above which one can violate the instrumental inequality** (5)**:** At $(\eta_a, \eta_b) = (0.8285, 1)$ the optimal states are maximally entangled state while at $(\eta_a, \eta_b) = (1, 0.667)$ we need an almost separable state.

the best critical detection efficiencies are obtained for states close to separability.

The effects of other sources of experimental errors

As shown in the main text, the expected quantum violation of the instrumental inequality is $\mathcal{I}_{\text{Q}} = 1 + 2\sqrt{2}$, achieved by a maximally entangled state of two qubits. In our experimental photonic setup, in order to prepare one of those states it is necessary to use a Spontaneous Parametric Down Conversion (SPDC)-type II source. It has been shown [10][11] that these sources suffer from two different kinds of noise: white noise and colored noise. Thus, the experimental state given by the mixture of these two noises can be modeled as:

$$\begin{aligned} \varrho_{noise} =& v|\phi^+\rangle\langle\phi^+| + \\ &+(1-v)\left[\lambda\frac{|\phi^+\rangle\langle\phi^+| + |\phi^-\rangle\langle\phi^-|}{2} + (1-\lambda)\frac{\mathbb{I}}{4}\right]. \end{aligned} \tag{22}$$

White noise is responsible for the appearance of the maximally mixed state and coloured noise for the appearance of $|\phi^-\rangle\langle\phi^-|$.

Considering this state and optimizing over the measurement settings for each value of v and λ we obtain the results shown in Fig. 5. The point marked in this figure represents the experimental violation expected from the characterization of our EPR source that corresponds to $v \approx 0.94$ and $\lambda \approx 0.33$ yielding $\mathcal{I}_{\text{Q}} = 3.643$. Since half wave-plates and fibers don't introduce significant noise we can consider this point as the theoretical expected violation for the experiment based on post-selection of data. Therefore, it's clear that our experimental result of $\mathcal{I}_{\text{Q}} = 3.621 \pm 0.023$ is in almost perfect agreement with the theoretical one.

In order to confirm also the Pockels Cell experimental results, we need to model the non-perfect efficiency of

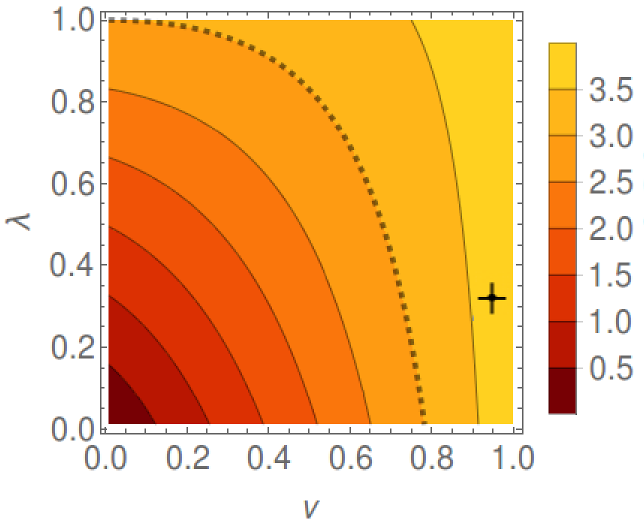

FIG. 5. **EPR source noise effect on inequality parameter:** In this graph is represented, by a scale of colors as showed in the label, the maximum values of $\mathcal{I}_Q$ for any v and λ according to the state in (22). The black cross denotes the estimated working point of our EPR source while the dashed line separates the region of violations (to the right) from the region of no-violation of the instrumental inequality (to the left).

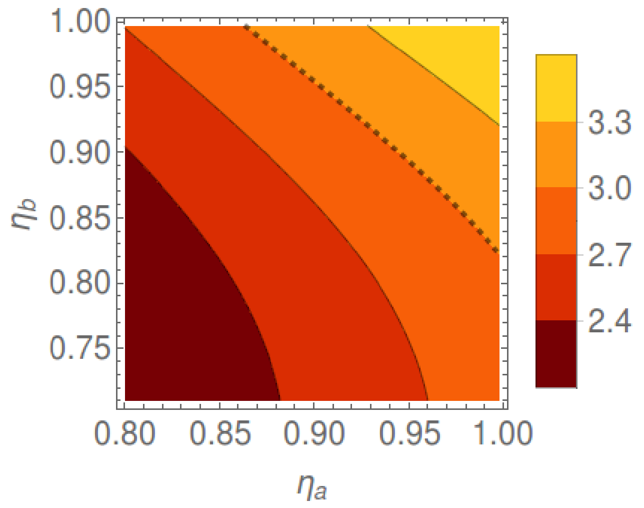

FIG. 6. **No-click and EPR source noise effect on inequality parameter:** Maximum violations reached in a no-click scenario by maximizing over the state and measurement settings considering the presence of colored and white noise at the working point of our EPR source. The magnitude of violation is represented by a scale of colors separated by contours. The dashed line separates the region where a violation occurs (on the right) from the region where $\mathcal{I}_Q$ is lower than the classical bound (on the left).

the crystal implementing σ_z. We thus have to take into account the possibility in which the Pockels Cell acts as identity instead of σ_z. This can be modeled by a Pockels Cell visibility v_{pc} that can be interpreted as the probability of not applying the σ_z transformation. Thus, the case when $a = 0$ (the case when the σ_z should be applied) can be computed as

$$p_Q(0, b|x) = \mathrm{Tr}\left[\left(M_0^x \otimes M_b^1\right) \varrho_{noise}^{pc}\right], \tag{23}$$

where

$$\varrho_{noise}^{pc} = (1 - v_{pc})\varrho_{noise} + v_{pc}\mathbb{I}^A \otimes \sigma_z^B \varrho_{noise}\mathbb{I}^A \otimes \sigma_z^B. \tag{24}$$

All other probabilities should be computed just as in equation (6) but considering a state given by ϱ_{noise}. We have evaluated experimentally the crystal visibility which was found to be $v_{pc} = 0.87$. Together with the other sources of errors we find the expected violation to be $\mathcal{I}_Q = 3.342$ which is in very good agreement with our experimental result of $\mathcal{I}_Q = 3.358 \pm 0.020$. We want to highlight that the previous result can be achieved also considering a POVM (Positive operator valued measure) instead of modifying the probability as done in (23). To show it, we can define such POVM by the following operators:

$$E_0^0 = v_{pc}|\tilde{0}\rangle\langle\tilde{0}| + (1 - v_{pc})|\not{0}\rangle\langle\not{0}| \tag{25}$$

$$E_1^0 = v_{pc}|\tilde{1}\rangle\langle\tilde{1}| + (1 - v_{pc})|\not{1}\rangle\langle\not{1}| \tag{26}$$

where $|\not{0}\rangle, |\not{1}\rangle$ are the eigenvectors of $\frac{\sigma_z - \sigma_x}{\sqrt{2}}$ while $|\tilde{0}\rangle, |\tilde{1}\rangle$ represent the eigenspace of $\frac{\sigma_z + \sigma_x}{\sqrt{2}}$. Replacing the projective measurements M_b^0 with eq. (25) and (26), we obtain again $\mathcal{I}_Q = 3.342$.

Now, we consider how the no-click events joined with EPR source noise (considered in the post-selection experiment) would affect the maximal violation achievable. To take into account no-click events and the possibility that the maximum value of $\mathcal{I}_Q$ is not always reached by maximally entangled state for all values of η_a and η_b, we modified the state in eq. (22) as following:

$$|\phi_\theta\rangle \equiv \cos\theta|\uparrow\uparrow\rangle + \sin\theta|\downarrow\downarrow\rangle \tag{27}$$

$$|\phi_\theta^\perp\rangle \equiv \sin\theta|\uparrow\uparrow\rangle - \cos\theta|\downarrow\downarrow\rangle \tag{28}$$

$$\begin{aligned}\varrho_{noise} =& v|\phi_\theta\rangle\langle\phi_\theta| + \\ &+(1-v)[\lambda\frac{|\phi_\theta\rangle\langle\phi_\theta| + |\phi_\theta^\perp\rangle\langle\phi_\theta^\perp|}{2} + (1-\lambda)\frac{\mathbb{I}}{4}]\end{aligned} \tag{29}$$

Fixing the values of λ and v (0.33 and 0.94 respectively), maximizing the violation over measurement settings and θ in the POVM scenario depicted in eq. (21) with $\eta_\uparrow^{a,b} = 1$ and $\eta_\downarrow^{a,b} = \eta_{a,b}$, contours in Fig. 6 were obtained.

Since the parameters λ and v, reported above, were estimeted exploiting the accidental counts correction method, all the previous analyzes are valid only in the case we compare our theoretical expectation values with the experimental ones where such correction was taken into account. Therefore, in order to perform a similar analysis to predict the violation values without correction, we have to just modify the state ϱ_{noise} adding a further term of white noise:

$$\begin{aligned}\varrho_{noise}^{noacc} =&\gamma\Bigg[v|\phi^+\rangle\langle\phi^+|+ \\ &+(1-v)\left(\lambda\frac{|\phi^+\rangle\langle\phi^+|+|\phi^-\rangle\langle\phi^-|}{2}+(1-\lambda)\frac{\mathbb{I}}{4}\right)\Bigg]+ \\ &+(1-\gamma)\frac{\mathbb{I}}{4}.\end{aligned} \tag{30}$$

where γ is a parameter which can be experimentally calculated as follows:

$$\gamma = 1 - \frac{\sum_{a,b} Acc_{a,b}}{\sum_{a,b} Coinc_{a,b}} \tag{31}$$

in Eq. (31) $Acc_{a,b}$ and $Coinc_{a,b}$ are, respectively, the accindental counts and the total coincidence counts observed by detectors associated to the a, b outcomes. From our data we have obtained $\gamma \approx 0.971$ which leads to the following theoretical expectation values:

$\mathcal{I}_Q = 3.537$, for the post-selection experiment.

$\mathcal{I}_Q = 3.245$, for the active feed-forward experiment.

Those results are again in agreement with the experimental values reported in the main text.

* rchaves@iip.ufrn.br

† fabio.sciarrino@uniroma1.it

[1] T. Christof and A. Löbel, "PORTA – POlyhedron Representation Transformation Algorithm," (2009).

[2] J. Barrett, N. Linden, S. Massar, S. Pironio, S. Popescu, and D. Roberts, "Nonlocal correlations as an information-theoretic resource," Phys. Rev. A **71**, 022101 (2005).

[3] S. Popescu and D. Rohrlich, "Quantum nonlocality as an axiom," Foundations of Physics **24**, 379–385 (1994).

[4] R. Chaves, R. Kueng, J. B. Brask, and D. Gross, "Unifying framework for relaxations of the causal assumptions in Bell's theorem," Phys. Rev. Lett. **114**, 140403 (2015).

[5] Alexei A Fedotov, Peter Harremoës, and Flemming Topsoe, "Refinements of pinsker's inequality," IEEE Transactions on Information Theory **49**, 1491–1498 (2003).

[6] Johannes Handsteiner, Andrew S. Friedman, Dominik Rauch, Jason Gallicchio, Bo Liu, Hannes Hosp, Johannes Kofler, David Bricher, Matthias Fink, Calvin Leung, Anthony Mark, Hien T. Nguyen, Isabella Sanders, Fabian Steinlechner, Rupert Ursin, Sören Wengerowsky, Alan H. Guth, David I. Kaiser, Thomas Scheidl, and Anton Zeilinger, "Cosmic bell test: Measurement settings from milky way stars," Phys. Rev. Lett. **118**, 060401 (2017).

[7] http://thebigbelltest.org/ .

[8] Rafael Chaves and Jonatan Bohr Brask, "Feasibility of loophole-free nonlocality tests with a single photon," Phys. Rev. A **84**, 062110 (2011).

[9] Philippe H. Eberhard, "Background level and counter efficiencies required for a loophole-free einstein-podolsky-rosen experiment," Phys. Rev. A **47**, R747–R750 (1993).

[10] Adán Cabello, Álvaro Feito, and Antía Lamas-Linares, "Bell's inequalities with realistic noise for polarization-entangled photons," Phys. Rev. A **72**, 052112 (2005).

[11] G. Cañas, J. F. Barra, E. S. Gómez, G. Lima, F. Sciarrino, and A. Cabello, "Detection efficiency for loophole-free bell tests with entangled states affected by colored noise," Phys. Rev. A **87**, 012113 (2013).